

GA-A26492

PLASMA STARTUP DESIGN OF FULLY SUPERCONDUCTING TOKAMAKS EAST AND KSTAR WITH IMPLICATIONS FOR ITER

by

J.A. LEUER, N.W. EIDIETIS, J.R. FERRON, D.A. HUMPHREYS, A.W. HYATT,
G.L. JACKSON, R.D. JOHNSON, B.G. PENAFLORE, D.A. PIGLOWSKI,
M.L. WALKER, A.S. WELANDER, S.W. YOON, S.H. HAHN, Y.K. OH,
B.J. XIAO, H.Z. WANG, Q.P. YUAN and D. MUELLER

JULY 2009



DISCLAIMER

This report was prepared as an account of work sponsored by an agency of the United States Government. Neither the United States Government nor any agency thereof, nor any of their employees, makes any warranty, express or implied, or assumes any legal liability or responsibility for the accuracy, completeness, or usefulness of any information, apparatus, product, or process disclosed, or represents that its use would not infringe privately owned rights. Reference herein to any specific commercial product, process, or service by trade name, trademark, manufacturer, or otherwise, does not necessarily constitute or imply its endorsement, recommendation, or favoring by the United States Government or any agency thereof. The views and opinions of authors expressed herein do not necessarily state or reflect those of the United States Government or any agency thereof.

PLASMA STARTUP DESIGN OF FULLY SUPERCONDUCTING TOKAMAKS EAST AND KSTAR WITH IMPLICATIONS FOR ITER

by

J.A. LEUER, N.W. EIDIETIS, J.R. FERRON, D.A. HUMPHREYS, A.W. HYATT,
G.L. JACKSON, R.D. JOHNSON, B.G. PENAFLO, D.A. PIGLOWSKI,
M.L. WALKER, A.S. WELANDER, S.W. YOON,* S.H. HAHN,* Y.K. OH,*
B.J. XIAO,† H.Z. WANG,† Q.P. YUAN† and D. MUELLER‡

This is a preprint of a paper to be submitted for
publication in IEEE Transactions on Plasma
Science.

*National Fusion Research Institute, Yuseong, Daejeon, Korea

†Institute of Plasma Physics, Chinese Academy of Sciences, Hefei Anhui, China

‡Princeton Plasma Physics Laboratory, Princeton, New Jersey

Work supported by
the U.S. Department of Energy
under DE-FC02-04ER54698
and DE-AC02-09CH11466

GENERAL ATOMICS PROJECT 30200
JULY 2009

Plasma Startup Design of Fully Superconducting Tokamaks EAST and KSTAR with Implications for ITER

J.A. Leuer, N.W. Eidietis, J.R. Ferron,
D.A. Humphreys, A.W. Hyatt, G.L. Jackson,
R.D. Johnson, B.G. Penaflor, D.A. Piglowski,
M.L. Walker, A.S. Welander

General Atomics
P.O. Box 85608
San Diego, California 92186-5608 USA
leuer@fusion.gat.com

S.W. Yoon, S.H. Hahn, Y.K. Oh
National Fusion Research Institute
Daejeon, Korea

B.J. Xiao, H.Z. Wang, Q.P. Yuan
Institute of Plasma Physics, Chinese Academy of Sciences
Hefei, China

D. Mueller
Princeton Plasma Physics Laboratory
Princeton, New Jersey

Abstract—Recent commissioning of two major fully superconducting shaped tokamaks, EAST [Y. Wan, et al., Proc. 21st IAEA Fusion Energy Conf., Chengdu, China, 2006] and KSTAR [Y. K. Oh, et al., Proc. 25th Symp. on Fusion Technology, Rostock, Germany, 2008, O8-3], represents a significant advance in magnetic fusion research. Key to commissioning success in these complex and unique tokamaks was (1) use of a robust, flexible plasma control system (PCS) based on the validated DIII-D design [B. G. Penaflor, et al., Proc. 6th IAEA Tech. Mtg. on Control, Data Acquisition and Remote Participation for Fusion Research, Inuyama, Japan, 2007]; (2) use of the TokSys design and modeling environment, which is tightly coupled with the DIII-D PCS architecture [J. A. Leuer, et al., Fusion Eng. Design, vol. 74, p. 645, 2005], for first plasma scenario development and plasma diagnosis; and (3) collaborations with experienced, internationally recognized teams of tokamak operations and control experts. We provide an overview of the generic modeling environment and plasma control tools developed and validated within the DIII-D experimental program and applied through an international collaborative program to successfully address the unique constraints associated with startup of these next generation tokamaks. The unique characteristics of each tokamak and the machine constraints that must be included in device modeling and simulation, such as superconducting coil current slew rate limits and the presence of nonlinear magnetic materials, are discussed, along with commissioning and initial operational results. Lessons learned from the startup experience in these devices are summarized with special emphasis on ramifications for ITER.

Keywords: *fusion, DIII-D, EAST, KSTAR, ITER, tokamak, first plasma, breakdown, plasma initiation*

I. INTRODUCTION

The startup of the EAST [1] and KSTAR [2] fully superconducting tokamaks and the beginning of the ITER [3] construction phase represent a new era in the international quest to harness fusion energy for power generation. These newly commissioned machines are the culmination of tremendous engineering, manufacturing and construction projects brought

about by dedicated teams of engineers and scientists with national commitments to advance the worldwide state of fusion energy research. Successful plasma startup in each of these machines was aided by international collaboration among the device teams and control and operations experts from General Atomics and Princeton Plasma Physics Laboratory (PPPL). Much of the success of this collaboration can be attributed to the flexibility of the DIII-D [4] plasma control system (PCS) [5], which was adapted in distinctly separate forms for use in EAST [6] and KSTAR [7]. The versatility of a suite of generic tokamak modeling tools, TokSys [8], within which the machines' startup scenarios were developed, was also key to the successful collaborations. In addition to software tools, the team provided physics operations and computer support, including experience with modeling, diagnosing and controlling the plasma using the PCS. Collaborating experts provided consistent support and rapid response, both on-site and remotely, throughout each of the first plasma campaigns.

Figs. 1 and 2 show original TokSys design basis geometry of the Experimental Advanced Superconducting Tokamak (EAST) and Korean Superconducting Tokamak Advanced Research (KSTAR) devices, respectively. Although the devices have distinct long-term missions, for the purposes of plasma startup, they have similar topology and dimensions. The figures show poloidal field (PF) coils, vacuum vessel and the design plasma separatrix. Unlike other major tokamaks (JET [9], JT60-U [10] and DIII-D [4]), these superconducting (SC) machines are planned to have independent power supplies driving each major coil. Each PF power system in both devices contains a four-quadrant power supply (PS) connected in series with a switchable resistor circuit. Administrative constraints on PS use during both first plasma campaigns include current, current ramp rate, and voltage limits maintained below PS hardware capabilities, as well as constraints on permitted operating quadrants. The switchable series resistors provide the high coil voltage needed for plasma breakdown and initial plasma current rise. The breakdown resistors are switched into the

circuit at $t=0$, and typically switched out of the circuit when plasma burnthrough is achieved and substantial plasma current (50–100 kA) is produced. During this initial resistor phase of the discharge, the PS is available to trim the resistor voltage waveforms to meet the scenario PF current requirements. Successful breakdown and initial plasma current rise requires pre-programming of the PF coil current scenario to generate both ohmic flux variation needed to driving plasma current and equilibrium field time history required for stable equilibrium evolution.

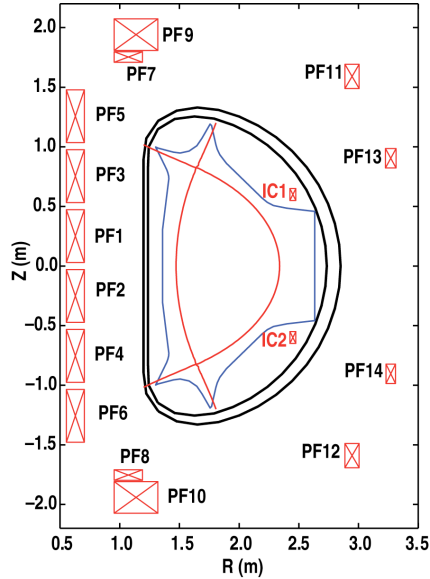


Figure 1. Reference EAST TokSys geometry showing SC PF coils, internal copper coils (ICs; not used for first plasma), vacuum vessel, limiter surface and reference EFIT [11] double-null plasma separatrix. PF7,9 and PF8,10 are connected in series-pairs. Additional internal components for divertor operation were added following the first plasma campaign.

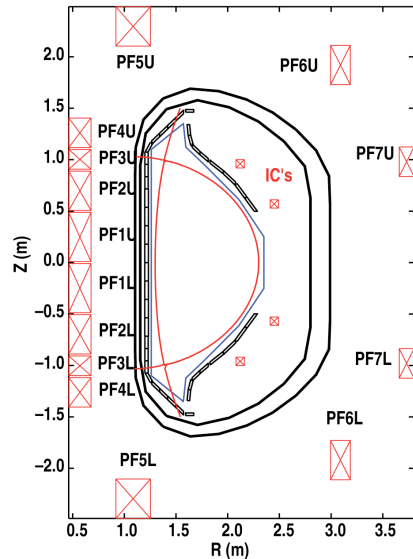


Figure 2. Reference KSTAR TokSys geometry showing SC PF coils, internal copper coils (ICs; not present for first plasma), vacuum vessel/passive structure (only partially installed for first plasma), limiter surface and reference EFIT [11] double-null plasma separatrix. All coils were connected in up/down series-pairs for first plasma campaign.

This paper describes the electromagnetic requirements for low voltage startup in tokamaks and presents the startup modeling efforts used to successfully design scenarios and initiate first plasma in KSTAR and EAST. Section II provides an overview and application of circular plasma formulas for development of the electromagnetic scenario and is an extension of the work performed earlier for ITER [12]. Section III presents results of first plasma commissioning and describes some of the control techniques utilized for first plasma operation in each device. Section IV provides a summary and contains general comments on lessons learned in the context of ITER.

II. PLASMA START-UP SCENARIO FORMULATION AND DESIGN

The basic criteria for plasma startup are based on early theoretical analysis of equilibrium conditions required for circular plasma formation in a tokamak [13]. Table I shows the circular plasma equilibrium equations utilized to establish linear plasma current and vertical field ramp rate and decay index requirements for a particular plasma. The loop voltage (equivalently the electric field) is the driving function for the plasma current rise as defined by the plasma circuit equation. This loop voltage is directly calculated as the flux change over the plasma area associated with the change in PF coil currents and passive structure eddy currents. Plasma resistive losses are characterized by an intrinsic loss coefficient C_{Res} , which is directly related to a transient Ejima coefficient C_{Ejima} [14] as shown in the bottom of Table 1. Generally, the plasma requirements are insensitive to other plasma parameters and this formulation provides a simple and robust description for developing the PF coil current scenario without the complexity inherent in the detailed physics of the plasma formation. This formulation, when coupled with experimental results on existing large-scale machines (JET [15], JT60-U [10] and DIII-D [16]), constitutes the

TABLE I. PLASMA STARTUP FORMULAS FOR CIRCULAR PLASMA (ADAPTED FROM [12,13])

	Formula	Reference
Electric field	$E_0 = -\frac{1}{2\pi R_0} \frac{d\phi_{pf}}{dt}$	$E_0 \geq 0.15$ V/m (ECH) ≥ 0.30 V/m (no ECH)
Central voltage	$V_0 = 2\pi R_0 E_0$	Definition
Current ramp rate	$i_p = \frac{(V_0 - V_{res})}{\mu_0 R_0 \hat{L}_p}$	$(V_0 - V_{res}) = V_0(1 - C_{res})$
Vertical field	$B_z = -\frac{\mu_0 I_p}{4\pi R_0} \left[\hat{L}_p + \beta + \frac{1}{2} \right]$	[13]
Radial field	$B_r = -n \frac{B_z}{R_0} [Z - Z_0]$	[13]

i_i = internal inductance (~ 1); β = dimensionless plasma pressure (~ 0.1);

n = decay index = $-\frac{R}{B_z} \frac{\partial B_z}{\partial R} \Rightarrow (0 < n < 3/2)$ [13]; κ =elongation,

$\frac{d\phi_{pf}}{dt}$ = Rate of change of flux from PF coils,

$$C_{Ejima} = \text{Ejima Coefficient [14]}, C_{res} = \frac{C_{Ejima}}{\hat{L}_p + C_{Ejima}}, \hat{L}_p = \left[\ln \left(\frac{8R_0}{a\sqrt{\kappa}} \right) + \frac{\ell_i}{2} - 2 \right]$$

basic elements needed to develop an appropriate electromagnetic scenario for plasma startup. The experimentally determined guidelines for ohmic electron cyclotron radio frequency (ECRF) startup are [15,16]:

$$\begin{aligned} E_\phi &\geq 0.3 \text{ V/m, [ohmic]} \\ E_\phi &\geq 0.15 \text{ V/m, [with ECRF]} \end{aligned} \quad (1)$$

$$\frac{E_\phi}{B_\perp / B_\phi} \geq 10^3 \text{ V/m} \quad (2)$$

where E_ϕ is the toroidal electric field, B_ϕ is the toroidal field, and B_\perp is the average poloidal field in the breakdown region.

The addition of ECRF for pre-ionization and plasma heating greatly assists plasma formation and burnthrough and allows for a reduction in the required electric field by approximately a factor of two [16]. Lower hybrid radio frequency (LHRF) heating, as is utilized in EAST, aids greatly in plasma burnthrough, but generally does not aid in pre-ionization, and is not as effective as ECRF [10] heating which is used in KSTAR for reduction of electric field requirements. Generally, the EAST electric field capability was approximately twice the minimum ohmic startup requirement at $E_{\phi\text{EAST}} \sim 0.6 \text{ V/m}$, while KSTAR, with its ECRF capability, was designed with $E_{\phi\text{KSTAR}} \sim 0.3 \text{ V/m}$ capability. Both design values represent a factor of two margin over predicted limits to account for design anomalies associated with startup of a new machine and are essentially identical to the criteria established many years ago for ITER [12].

The overall methodology and software used to develop a machine-dependent scenario for plasma startup is delineated in [12,17]. Here we provide an overview of the procedure and examples of its use. For the resistor driven breakdown used in KSTAR and EAST, and planned for ITER, the primary design must define the initial magnetization (IM) coil current state and the resistor values needed to drive the fields required for plasma evolution. The power supply system is then available to fine-tune the coil voltages to best match the prescribed coil cur-

rent scenario and ultimately the plasma requirements. Eddy currents in the vessel must be included in the analysis since they substantially alter the fields in the early phases of plasma formation. The design is constrained by restrictions placed on the allowable coil currents, voltage, and coil current ramp rate based on particular machine limitations. The design is done with an optimization routine that includes the influence of eddy currents [12] and allows for inclusion of all superconducting magnet constraints [17].

Scenario development consists of determination of the IM state currents based on a least square minimization technique, along with specification of the resistor, and voltage and current waveforms required. These latter are determined by an eigenmode analysis of the circuit equations coupled to a linear quadratic programming methodology to match plasma evolution targets expressed in Table I and include constraints associated with PF coil system such as current, voltage and coil ramp rate limits. The routines all are formulated utilizing the TokSys [8] environment specific to each device. Fig. 3 shows examples of the initial IM state and target/simulated plasma vacuum field trajectories based on the optimized breakdown resistor scenario developed for EAST first plasma. Commissioning limitations included in the scenario development were primarily current and current ramp rate limits. The IM state current produced approximately 3 Vs of flux (double swing $\sim 6 \text{ Vs}$) [17]. The KSTAR commissioning included much more restrictive limits on PF coil currents and overall current swing capability. Overall Nb_3Sn PF magnets have a tremendous flux production capability; however, for commissioning, PF current and current swing capability was constrained by administrative, zero crossing, and site power limitations. For KSTAR two IM states were investigated: “conventional” with a coil current distribution that decreases from the inboard solenoid coils to the outside PF coils and “dipole” with approximately equal current magnitudes in the PF coils but with the outer two coils containing equal and opposite current in order to cancel their large fields at the plasma null location. Fig. 4 compares the two configurations optimized to produce 1 Vs flux at the breakdown

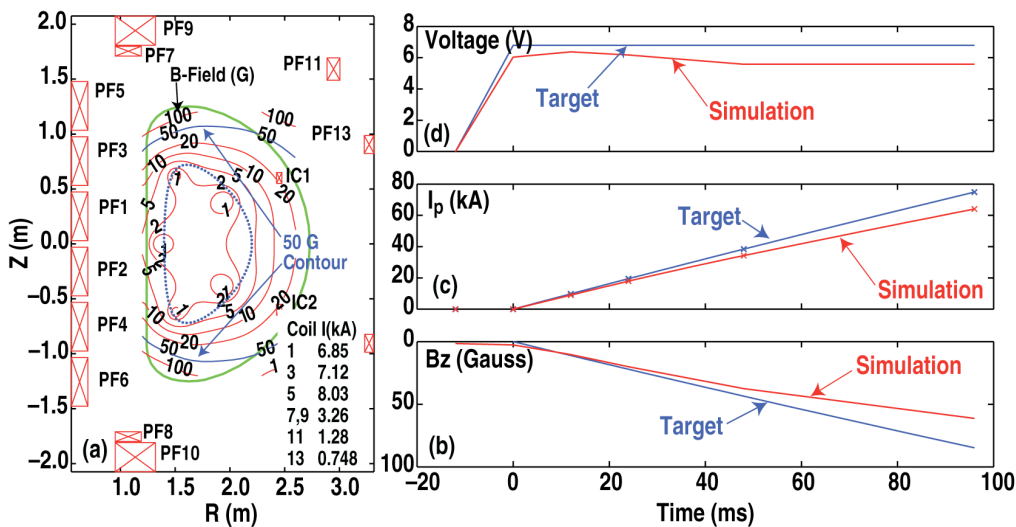


Figure 3. EAST Initial magnetization (IM) current state and design plasma scenario evolution for optimized resistor operation. IM PF coil currents and resulting B-field contours are shown in (a); solid blue contour shows 50 G level. Target and simulated waveforms are shown for the optimized resistor trajectory in (b) plasma loop voltage, (c) plasma current, and (d) vertical B-field. The IM state produces an initial flux state of 3 Vs in the plasma region [17].

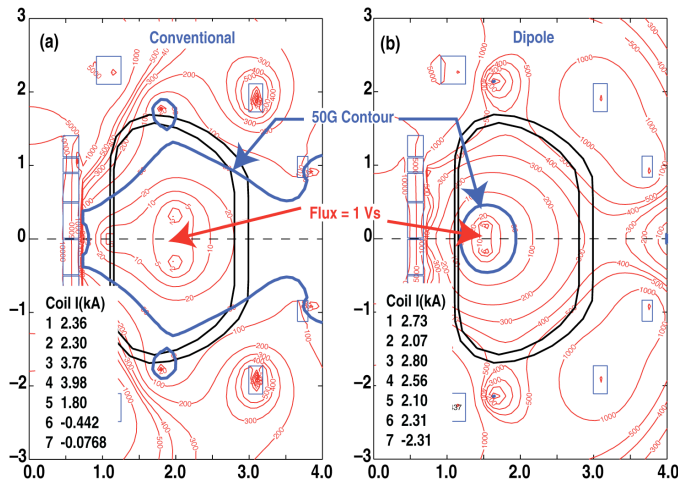


Figure 4. Early KSTAR IM state comparing (a) “conventional” and (b) “dipole” current configurations. Both configurations are designed to give an initial central flux of 1 V-s and minimum B-field in the breakdown region. Blue contour compares the 50 G contour for each configuration.

the environment provides direct connection to the PCS through generation of model based simulation servers (simservers) and allows detailed simulation of the PCS/Power Supply/Plasma system [19]. Fig. 5 shows the architecture of this simulation environment in a schematic form. Model development and scenario and controller design are accomplished in the upper blocks. Once controller and scenario design are prescribed and the controller implemented within the PCS, a complete closed loop simulation of the PCS/Model based simserver can run with functionality identical to that of the actual PCS controlling the tokamak (middle boxes). The simserver can contain a simple vacuum model or a linearized plasma model based on an EFIT equilibrium [12]. PCS interface, data acquisition storage and visualization methods are identical to that of an actual plasma discharge. This environment allows debugging of the entire system prior to operation on the tokamak and was indispensable in allowing for rapid startup of the SC machines.

KSTAR startup was complicated by the nonlinear magnetic behavior associated with the Incoloy 908 jacket material used in construction of the Nb₃Sn superconductors (SC) [2]. This material has a magnetic permeability of approximately 10 and a saturation magnetization equivalent to 1T, which is about one-half the value of iron. Prior to first plasma operation, substantial finite element (FE) analysis was performed to quantify its influence on the PF coil system and the magnitude of stray fields expected in the plasma. Preliminary estimates of the impact of Incoloy 908 indicated that single-coil inductance increases by more than 50% at low PF current levels (unsaturated). At higher currents, as different parts of the coil reach the saturated state, nonlinear behavior between PF current and B-field projections is predicted. Fig. 6 shows the magnetization state of the PF coil Incoloy 908 from the FE analysis of the system using the IM PF current state. The colored PF coil contours correspond to an effective magnetization (based on fraction of Incoloy in coil) with magnitude shown in the color bar. Only PF1-5 contain Incoloy 908. The TF coil is assumed to be saturated in the toroidal direction and its magnetization M is assumed to be zero in the analysis. Results show that a majority of the inner PF coils are saturated at the level of currents associated with the IM state. However, the field is shown to change sign as represented by the M_z profiles across PF1 and PF5 as depicted in the sub-figures. Accordingly different parts of the coil are in various stages of saturation and at different locations on the nonlinear region of the Incoloy 908 B-H curve. This greatly exacerbates the computation of plasma fields over similar computations in conventional tokamaks.

While the impact of Incoloy 908 magnetization in and near the magnets is substantial, the overall impact in the plasma region was determined to be of order 10s of Gauss. In addition, this field was reasonably uniform, primarily in the vertical direction, and is easily compensated for by using a modified IM state during startup. The influence of the Incoloy 908 adds to the complexity of B-field evaluation and magnetic diagnostic calibration and will require special modeling programs going forward to quantify its influence. Plasma reconstruction (e.g. EFIT [11]) becomes much more difficult; however, as part of the commissioning phase work, methods were developed to include the gross influence of Incoloy 908 in the nominal TokSys vacuum reconstruction routines.

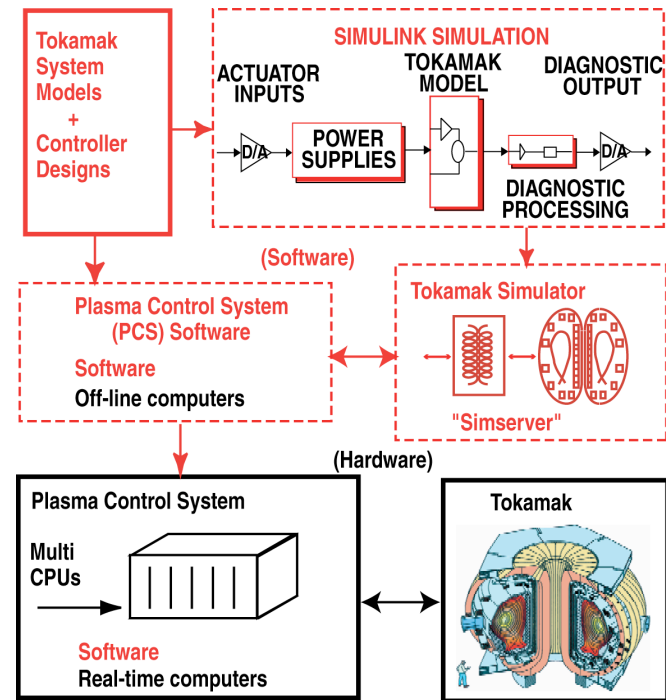


Figure 5. TokSys [8] environment including modeling environment shown in top boxes, model based, closed loop simulation environment shown in middle boxes and actual PCS/Tokamak closed loops system is schematically shown in the bottom two boxes. Red = software and black = hardware.

location. The conventional configuration generates a much larger null than the dipole but has much higher peak currents. Based on KSTAR current and power limits, the dipole configuration is capable of providing more flux and ultimately more plasma current. During actual plasma operations the IM states were modified to reflect additional machine constraints, including the influence of nonlinear magnetic materials [18].

Tools for scenario design and other plasma analysis were developed within the TokSys environment [8], which is tightly coupled to the internationally utilized DIII-D plasma control system (PCS) [5]. Along with the extensive analysis capability,

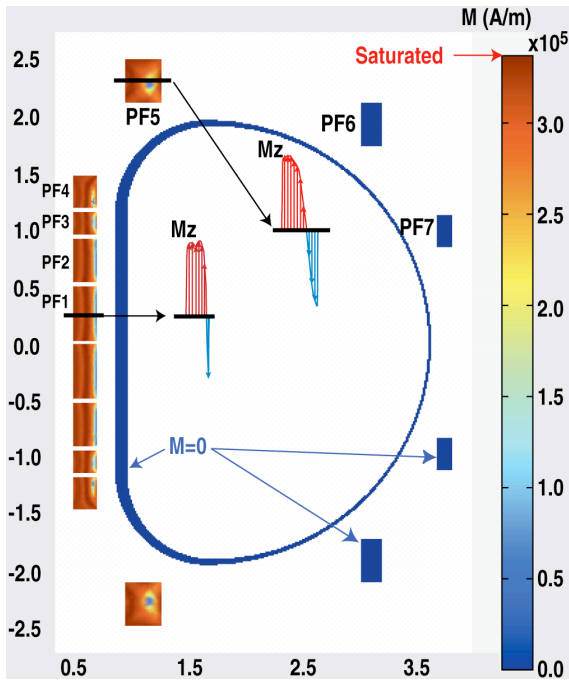


Figure 6. Magnetization contours based on FE analysis of KSTAR PF magnets with IM currents in presence of nonlinear Incoloy 908. Shown are the PF and TF coil FE geometry. In simulation, PF1-5 contain approximately 40% Incoloy 908. Outer PF coils contain no 908 and TF coil is assumed saturated in the toroidal direction and accordingly has $M=0$ in the model. A majority of the Incoloy 908 PF coils are saturated from the IM state currents and have an effective magnetization representative of an equivalent 1T component averaged over area. Actual distribution of the Z component of the magnetization is shown for PF1 and PF5 in the detailed cross sections and is shown to change sign over the cross section.

III. FIRST PLASMA RESULTS

Both SC devices were very successful in their commissioning campaigns and met all objectives delineated for first plasma operation. First plasma in EAST was achieved on the first official day of plasma startup and was a result of the previously described scenario development, extensive simulation and machine testing, as well as the dedicated effort of the EAST and collaborator team [1]. These initial discharges exceeded the administrative targets for first plasma current amplitude and were followed by steady increases in current and successful pulse extension. Fig. 7 shows plasma current and loop voltage waveforms for first plasma generation [6,20,21]. A peak loop voltage of 5.5 V and ramp rates of 0.5 MA/s are in good agreement with design based scenario results. Fig. 8 shows the target PCS PF current and actual current waveforms for the first plasma (shot 1144). During the resistor phase ($t < 50$ ms) the PCS was operated in a voltage control mode with incremental \pm voltage superimposed onto the resistor voltage to regulate the current to best match the optimum current targets. Following the breakdown phase ($t > 50$ ms), the resistors were switched out of the system and PF coil current was feedback controlled by the PCS to best match the targets. The divergence of the actual currents from the targets was a result of differences in the power supply response characteristics from the design assumptions. Small modifications of the PF current trajectories allowed for better plasma centering and allowed plasma

currents to reach 200 kA with discharges longer than 1 s (shot 1149).

The KSTAR first plasma campaign also exceeded all plasma commissioning phase requirements. Substantial testing was performed to delineate the best scenario based on uncertainty introduced by the nonlinear magnetic material (Incoloy 908) within the SC coils [18]. Both the conventional and dipole configurations were developed. Fig. 9 shows first plasma (shot 794) current and loop voltage time history using the conventional IM configuration and using only PF coil current control. Also shown in the figure is a waveform generated later in the campaign using the dipole configuration (shot 1216) and using feedback control of plasma current and radial position (I_p , R_p). Utilizing second harmonic ECRF pre-ionization and heating (500 kW, 84 GHz gyrotron [22]) the conventional configuration produced currents in the range of 100 kA using electric fields slightly below the reference $E = 0.3$ V/m. The dipole configuration produced slightly higher plasma current owing to its increased capability of flux generation and provided better control owing to the increase current in the outer PF coils (PF 6,7) [18].

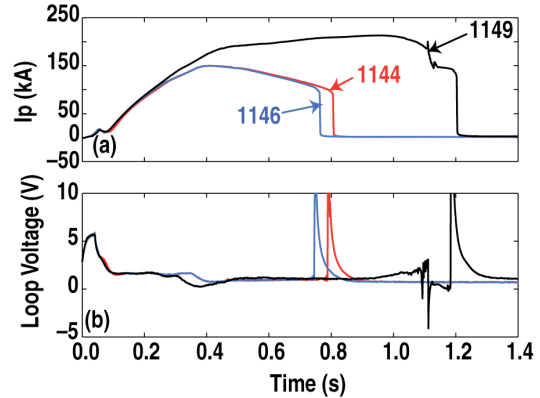


Figure 7. Plasma current time history for several shots during the first day of EAST plasma operations. Figures show: (a) plasma current and (b) loop voltage for several early shots (1144, 1146 and 1149). Loop voltage, as determined by the inner flux loop, peaks at 5.5 V at plasma breakdown [17].

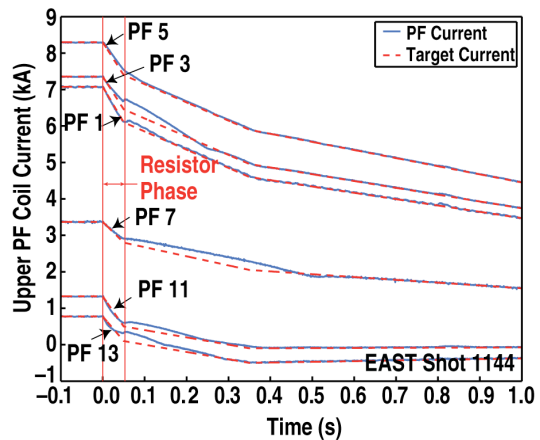


Figure 8. PF coil current target and actual experimental waveforms for first EAST plasma (shot 1144). IM state represents the current before $t = 0$; resistor phase is $0 < t < 50$ ms; PF current control is active for $t > 50$ ms. Symmetric PF coil currents below the midplane have approximately identical waveforms [17].

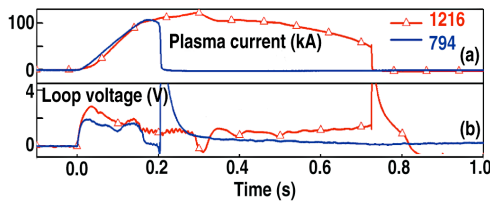


Figure 9. Plasma current time history for several shots during KSTAR’s first campaign. Figures show: (a) plasma current and (b) loop voltage for first plasma (794) using conventional configuration and shot 1216 which used the dipole configuration and had I_p , R_p feed back control. Loop voltage peaks at 2.5-3 V at plasma breakdown and is commensurate with the $E < 0.3$ V/m objective of KSTAR commissioning phase [18].

Following first plasma generation using only PF coil current scenario evolution, both machines quickly improved performance by implementing plasma feedback control [6,7]. The general structure and flexibility of the PCS [6,7,17,23] and modeling and data analysis tools available in the TokSys environment provided all the necessary components needed to rapidly control I_p and R_p in each campaign. Estimators for R_p , Z_p were constructed based on linear combinations of all input diagnostics signals to the PCS. As an example, Fig. 10 shows the R_p linear estimator developed for KSTAR first plasma based on signals from the closest midplane inside/outside B-probes in the system. The actual PCS implementation utilized these signals normalized by plasma current and with PF coil signals removed from the estimation. This latter technique is important for new machines like KSTAR and EAST in that the coil currents are typically the best diagnosed signals in the system. Fig. 11 shows radial position control developed early in the KSTAR I_p , R_p control part of the campaign. Fig. 12 shows Z_p control achieved late in the EAST campaign utilizing a programmed variation in vertical position to determine dynamic characteristics. The lag in control is associated with power supply dynamics. In EAST, testing was performed to determine the elongation limit associated with vertical stability using only the SC coils. As expected, vertical displacement events (VDEs) were observed close to the natural elongation limit, $\kappa \sim 1.15$. Owing to the limits imposed by the SC magnet/PS system, both machines must utilize internal coils to obtain diverted plasmas. Diverted plasmas have been obtained in EAST [24] and are planned for KSTAR in 2010 using internal coils. For both machines good I_p , R_p control was essential in obtaining optimal performance in their circular plasma operations.

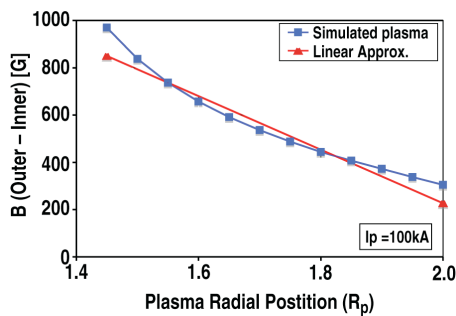


Figure 10. Development of the KSTAR plasma radial position estimation based on inner and outer midplane located B-probes. Estimated response from plasma motion (in blue), red shows the linear estimate implemented in the PCS.

IV. SUMMARY AND LESSONS LEARNED FOR ITER

Both EAST and KSTAR have generated a wealth of new knowledge with regard to the startup of such tokamaks in general, and SC tokamaks in particular. Some important lessons for ITER arise from these startup experiences. Startup of SC devices is tractable using available modeling and design methods and generally follows design predictions. In particular, electromagnetic startup scenario development using the standard circular plasma formulation is accurate and adequate for first plasma commissioning. Startup of tokamaks using individually powered PF coils with initiation voltage utilizing switched resistors is highly effective and provides a robust startup method. The electric field requirements of ITER ($E_\phi = 0.3$ V/m) provide a factor of two margin over the minimum required in existing, well characterized machines and is appropriate for startup with sufficient ECRF power. Values approaching 0.6 V/m are desirable without ECRF assist. Rapid success in commissioning was a result of (1) utilization of a well developed PCS, (2) utilization of validated modeling and analysis tools developed on existing machines and tightly integrated with the PCS and 3) the ability to test all aspects of plasma control and modeling in closed loop with the PCS. A similar environment will be essential for ITER. Collaboration with an international team of startup experts from existing machines (DIII-D and NSTX) greatly expedited startup and provided a high level of confidence in achieving the commissioning goals. Internal coils are needed to obtain diverted operation using PF magnet systems and power supply constraints typical of those used in the new SC tokamaks. ITER has added internal coils and this seems appropriate in light of this experience with KSTAR and EAST. KSTAR, with its use of Nd_3Sn coils, has developed superconducting technology

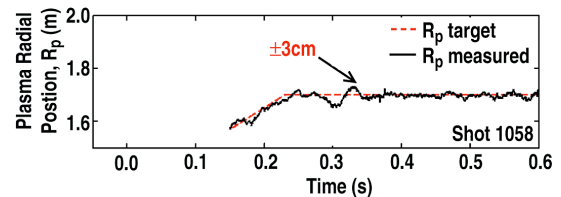


Figure 11. KSTAR Radial plasma position R_p relative to target for shot 1058 [7].

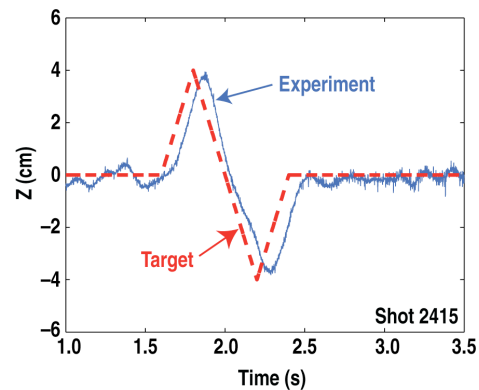


Figure 12. EAST vertical plasma position Z_p response to a slow vertical triangular target for shot 2415. A time lag of order 50 ms is seen between target and experiment and primarily is a result of power supply properties. [17].

directly applicable to ITER. Much of the knowledge developed during KSTAR's evolutionary process of dealing with the nonlinear material (Incoloy 908) is expected to be valuable to the ITER project, which is expected to utilize nonlinear material in TF ripple reduction inserts and test blanket modules. This knowledge will also be valuable beyond ITER since ferromagnetic materials are promising candidates for actual power plant construction. Finally, there are many severe limitations associated with SC devices, some of these only associated with commissioning. All metal walls and low bake temperatures were common in both experiments and did impact startup. However, use of boronization in EAST and long bake times in KSTAR helped alleviate their impact and impurity conditions did not significantly impede commissioning in either device. In the years to come, both machines are expected to address many issues relevant to ITER and, more generally, are expected to substantially increase the knowledge base necessary for development of fusion energy power plants.

ACKNOWLEDGMENT

This work was supported by the US Department of Energy under DE-FC02-04ER54698 and DE-AC02-09CH11466.

REFERENCES

- [1] Y. Wan, et al., Proc. 21st IAEA Fusion Energy Conf., Chengdu, China, 2006.
- [2] Y. K. Oh, et al., Fusion Engin. Design vol. 84, p. 344, 2009.
- [3] K. Ikeda, Nucl. Fusion, vol. 47(6), preface, 2007.
- [4] L. G. J. Davis, J. Vac. Sci. Technol. A, vol. 1, p. 1319, 1983.
- [5] B. G. Penaflor, et al., Proc. 25th Symp. Fusion Tech., Rostock, Germany, 2008, to be published in Fusion Eng. Design.
- [6] B. J. Xiao, Proc. 6th IAEA Tech. Mtg. on Control, Data Acquisition and Remote Participation for Fusion Research, Inuyama, Japan, 2007.
- [7] S-H. Hahn, et al., "Plasma control system for 'Day-One' operation of KSTAR tokamak", Fusion Engin. Design, 2009, doi:10.1016/j.fusengdes.208.12.082.
- [8] D. A. Humphreys, et al., Nucl. Fusion, vol. 47, p. 943, 2007.
- [9] K. J. Dietz, et al., in Proc. 6th Intl. Conf. on Plasma Surface Interactions in Controlled Fusion Devices, Nagoya., J. Nucl. Mater., vol. 128, p. 10, 1984.
- [10] R. Yoshino and M. Seki, Plasma Phys. Control. Fusion, vol. 39, p. 205, 1997.
- [11] L. L. Lao, et al., Nucl. Fusion, vol. 25, p. 1421, 1985.
- [12] J. A. Leuer et al., Proc. 15th IEEE/NPSS Symp. on Fusion Engineering, Hyannis, 1993 (Institute of Electrical and Electronics Engineers, Inc., Piscataway, New Jersey, 1994) vol. 2, p. 629.
- [13] V. S. Mukhovatov and V. D. Shafranov, Nucl. Fusion, vol. 11, p. 605, 1971.
- [14] S. Ejima, et al., "Volt-Second Analysis and consumption in Doublet III plasma," Nucl. Fusion, vol. 22, no.10, p. 1313, 1982.
- [15] A. Tanga, et al., *Tokamak Start-up* (Plenum Press, New York, 1986) p. 159.
- [16] B. Lloyd, et al., Nucl. Fusion, vol. 31, p. 2031, 1991.
- [17] J. A. Leuer et al., submitted to: Fusion Science and Technology.
- [18] Y. K. Oh, et al., "Commissioning and initial operation of KSTAR superconducting tokamak," Fusion Engin. Design, 2009, doi:10.1016/j.fusengdes.2008.12.009.
- [19] J. A. Leuer, et al., Fusion Engin. Design, vol. 74, p. 645, 2005.
- [20] Yuanxi Wan, et al., Proc. 21st IAEA Fusion Energy Conf., Chengdu, 2006 (International Atomic Energy Agency, 2006) OV/1-1; http://www-pub.iaea.org/MTCD/Meetings/FEC2006/ov_1-1.pdf
- [21] P. Weng, et al., Proc. 21st IAEA Fusion Energy Conf., Chengdu, 2006 (International Atomic Energy Agency, 2006) FT/P7-11; http://www-pub.iaea.org/MTCD/Meetings/FEC2006/ft_p7-11.pdf
- [22] Y.S. Bae, et al., "Status of KSTAR electron cyclotron heating system," Fusion Sci. Technol., vol. 52, p. 771, 2007.
- [23] B. G. Penaflor, et al., Proc. 6th IAEA Tech. Mtg. on Control, Data Acquisition and Remote Participation for Fusion Research, Inuyama, Japan, 2007.
- [24] B. J. Xiao, et al., Proc. 34th European Conf. Plasma Physics, Warsaw, 2007 edited by Pawel Gasior and Jerzy Wolowski (European Physical Society, 2007) vol. 31F, paper O4_014; http://epsppd.epfl.ch/Warsaw/pdf/O4_014.pdf